J. Phys. B: At. Mol. Opt. Phys. 27 (1994) 429–446. Printed in the UK

Atomic data for opacity calculations: XX. Photoionization cross sections and oscillator strengths for Fe II

Sultana N Nahar and Anil K Pradhan

Department of Astronomy, The Ohio State University, Columbus, OH 43210, USA

Received 17 March 1993, in final form 12 October 1993

Abstract. Large scale *ab initio* calculations for the radiative data of Fe II have been carried out in the close coupling (CC) approximation employing the R-matrix method and a target state expansion consisting of 83 LS terms of Fe III. All bound states of Fe II with $n \leqslant 10$ and $l \leqslant 7$ are considered. The results include 1301 bound states in LS coupling, oscillator strengths for 35 941 transitions among the bound LS states, and detailed photoionization cross sections for all bound states. Autoionizing resonances, as well as the coupling to excited core states, enhance the photoionization cross sections substantially. The calculations of oscillator strengths have been extended beyond the requirement of the Opacity Project to include a large number of fine structure transitions in Fe II, using an algebraic transformation of the LS coupled line strength and the observed energies. The present f-values compare favourably with available experimental values and the calculations by Kurucz. However, the present results differ considerably from earlier 16-state R-matrix calculations and the new radiative data yield Rosseland mean opacities that are 50% higher. Some special features in the monochromatic opacity spectra of Fe II are also noted.

1. Introduction

Under the auspices of the Opacity Project (OP; Seaton 1987) *ab initio* calculations for accurate atomic radiative data for essentially all astrophysically abundant atoms and ions have been carried out by international collaborators, as reported in previous papers in this ADOC (Atomic Data for Opacity Calculations) series. The present work involves large scale computations for Fe II in the close coupling approximation, employing the R-matrix method as adapted for the OP. With many closely spaced energy levels, Fe II is a complex atomic system of 25 electrons where the electron correlation effects play a very important role. Recently Sawey and Berrington (1992) have reported R-matrix calculations for a few iron ions. Their Fe II calculations employed a close coupling (CC) expansion including only the states dominated by the $3d^6$ ground configurations of the residual ion or the 'target' ion Fe III. As we show in the present, much more extended work, it is necessary to also include a large number of additional terms in the eigenfunction expansion, dominated especially by the excited $3d^5 4s$ and the $3d^5 4p$ configurations, in order to obtain accurate radiative parameters. The aim of the present R-matrix close coupling calculations of Fe II is to take into account all the important states of Fe III in the wavefunction expansion and obtain more accurate radiative data for energy levels, oscillator strengths and photoionization cross sections. The importance of such calculations and a summary of theoretical details can be obtained in the first two papers of the ADOC series (Seaton 1987, Berrington *et al* 1987). In an earlier brief report

(Le Dourneuf *et al* 1993), we reported the first detailed calculation, with autoionizing resonances and channel coupling effects, for the photoionization of the states with the ground state symmetry ^{6}D. The present report is a complete account of the comprehensive calculations including 90 total Fe II symmetries, and photoionization of all bound states up to $n \leqslant 10$ and $l \leqslant 7$ and oscillator strengths of all possible bound–bound transitions among the 1301 computed states.

In addition to the extensive *LS* coupling calculations for the OP calculations, we also obtain fine structure oscillator strengths for Fe II through an algebraic transformation of the *LS* multiplet line strengths and using observed spectroscopic energies. Most of the resulting fine structure *f*-values compare favourably with available experimental data, and rather better than those calculated by Kurucz (1981) using semi-empirical methods†. At present the data set by Kurucz is the only available source of Fe II *f*-values for most applications where a large number of transitions need to be considered. The present approach yields *f*-values for all transitions between the fine structure components of the dipole allowed *LS* multiplets, given the observed energies of the individual components. Thus a reasonably complete data set for the large number of Fe II *f*-values is obtained.

2. Target states

Following the convention of collision theory, we refer to the ion in the e+ion system as the 'target' ion (also, as the 'core' or the 'residual' ion following photoionization). The importance of accurate target representation in CC calculations is to be emphasized as the necessary first step. For the CC calculations for Fe II we obtain the target eigenfunctions for Fe III using the SUPERSTRUCTURE program by Eissner *et al* (1974) based on a scaled Thomas–Fermi–Dirac potential and configuration interaction (CI) wavefunctions. Given the number of states needed in the calculations, the atomic structure calculations are rather complicated since proper account needs to be taken of the CI effects, while the total number of configurations must be kept small to minimize, as much as possible, the memory of the CPU requirements. The task was found to be particularly difficult and time consuming for Fe III due to the large number of target states considered. The principal configurations (i.e. whose terms are explicitly included in the CC expansion) are: 3d^6, 3d^{5}4s and 3d^{5}4p. It might be noted here that it is the dipole core transitions between the even and the odd parity configurations that give rise to the well known photoexcitation-of-core (PEC) resonances in photoionization cross sections (Yu and Seaton 1987, Nahar and Pradhan 1991). The PEC resonances were not considered in the earlier work by Sawey and Berrington (1992) since the excited configurations were not included. As the 3d shell plays the dominant role in electron correlation, the correlation configurations are constructed mainly with respect to variations in the 3d orbital and excitations involving the 3d electrons. In addition, important improvements in the accuracy of the Fe III energies and oscillator strengths were achieved by introducing a correlation configuration with the 4d orbital (which increased the optimization time considerably). The final configuration list and the

† *f*-values given in this paper correspond to the most recent gf values calculated by him which were obtained from him by private communication.

Thomas–Fermi scaling parameters λ_{nl}, are given in table 1. The choice of the target states actually included in the CC calculations was somewhat independent of the target optimization since all 136 *LS* terms dominated by the three principal configurations, $3d^6$, $3d^54s$ and $3d^54p$, are well represented with the choice of the target in table 1. We include up to 83 terms in the present Fe II calculations. In particular we include all odd parity terms dominated by $3d^54p$ that are linked via dipole transitions to the ground state ^5D to take account of strong PEC resonances in the photoionization cross sections.

Table 1 compares the energies of the 83 terms of Fe III with the observed values (Sugar and Corliss 1985, Moore 1952). It may be noted that three calculated singlet terms: $3d^6$ (^1D, ^1S), $3d^5\ ^2S4s\ ^1S$, have not been observed. Comparison of the calculated target energies with the observed energies shows agreement within 10% for most of the states, the largest discrepancy being about 18% for the $3d^6\ ^1I$ state.

Over 300 dipole oscillator strengths were obtained from SUPERSTRUCTURE for the *LS* target states dominated by the $3d^6$, $3d^54s$ and $3d^54p$ configurations. These oscillator strengths show agreement between the length and the velocity forms within 15% for most of the transitions in Fe III, further confirming the overall accuracy of the large set of the target eigenfunctions.

In table 1, the notations O, S, Q and D in the target state column specify that the corresponding Fe III state couples to octet, sextet, quartet or doublet symmetry of the e+ion system, $SL\pi$, of Fe II respectively. Thus there are 2 O, 21 S, 58 Q and 62 D such terms of Fe III that are in the target expansion for radiative calculations of octet, sextet, quartet and doublet states of Fe II. In table 1, the number next to each notation of O, S, Q and D is the energy degeneracy number for that state. This will be explained in the following section.

3. Computations and calculations for the radiative data

As in the case of all OP work, the present computations have been carried out in *LS* coupling, that is, relativistic effects are not taken into account. Since Fe II is a singly charged ion, it has been assumed that *LS* coupling would provide a good approximation for the radiative data. All bound states, denoted as S_tL_tnl, where S_tL_t is a target state, and $n \leqslant 10$ and $l \leqslant 7$, are considered for the radiative data.

Each excited target state S_tL_t of the ion is the series limit for the Rydberg series $S_tL_t\nu l$ of the $(N+1)$ electron system, where ν is the effective quantum number of the $(N+1)$th electron. These are pure bound states if they lie below the first ionization threshold, but those that lie above the first ionization threshold are usually quasibound states and manifest themselves through autoionizing resonances in the photoionization cross sections (some states above the first ionization threshold may be pure bound states in *LS* coupling if they are forbidden to autoionize into the corresponding continua). These Rydberg resonances repeat the pattern for each increment of ν. As ν increases, the resonances get narrower and numerical resolution becomes difficult. To obviate the problem, we employ a constant mesh in ν, for each interval ν and $\nu+1$, to fully delineate the Rydberg resonances up to $\nu=10$ with a mesh interval of $\Delta\nu=0.01$. The region $10<\nu\leqslant\infty$, that we term as the QDT region, corresponds to a small energy region which is treated through quantum defect theory (QDT) using the Gailitis averaging method (e.g. Nahar and Pradhan 1991).

For closely spaced target states, as in the case of Fe III, the QDT region of different target states may overlap. Such target states with overlapping QDT regions are treated

Table 1. Calculated (cal) term energies of Fe III (configurations $3d^6$, $3d^54s$ and $3d^54p$) and comparison with the observed (obs) energies. The energies, in Ry, are relative to the $3d^6\ ^5D$ ground state. *The three states, $3d^54s\ ^1S$, $3d^6\ ^1D$ and $3d^6\ ^1S$, are unobserved. The notation* O, S, Q and D in the target state column specifies the coupling to the octet, sextet, quartet and doublet symmetries of Fe II respectively. The number next to them represents the degeneracy index (see text). The spectroscopic and correlation configurations for Fe III and the values of scaling parameter λ_{nl} for each orbital in the Thomas–Fermi potential are also given.

	State		Energy Obs.	Energy Calc.	Target states	
1	$3d^6$	^5D	0.0	0.0	[S1	Q1]
2	$3d^6$	$^3P2$	0.1826	0.1810	[Q2	D1]
3	$3d^6$	^3H	0.1845	0.2163	[Q3	D2]
4	$3d^6$	$^3F2$	0.1972	0.2105	[Q3	D2]
5	$3d^6$	^3G	0.2263	0.2537	[Q3	D2]
6	$3d^5(^6S)4s$	^7S	0.2742	0.2728	[O1	S2]
7	$3d^6$	^1I	0.2766	0.3246	[D3	]
8	$3d^6$	^3D	0.2805	0.3037	[Q4	D3]
9	$3d^6$	$^1G2$	0.2815	0.3021	[	D3]
10	$3d^6$	$^1S2$	0.3172	0.3190	[	D3]
11	$3d^6$	$^1D2$	0.3263	0.3460	[	D3]
12	$3d^5(^6S)4s$	^5S	0.3736	0.4167	[S3	Q5]
13	$3d^6$	^1F	0.3909	0.4295	[	D4]
14	$3d^6$	$^3P1$	0.4556	0.4900	[Q6	D5]
15	$3d^6$	$^3F1$	0.4580	0.4985	[Q6	D5]
16	$3d^6$	$^1G1$	0.5214	0.5738	[	D6]
17	$3d^5(^4G)4s$	^5G	0.5783	0.5995	[S4	Q7]
18	$3d^5(^4P)4s$	^5P	0.6061	0.6466	[S5	Q8]
19	$3d^5(^4D)4s$	^5D	0.6358	0.6730	[S5	Q8]
20	$3d^5(^4G)4s$	^3G	0.6444	0.6957	[Q9	D7]
21	$3d^5(^4P)4s$	^3P	0.6724	0.7438	[Q9	D7]
22	$3d^5(^4D)4s$	^3D	0.7019	0.7691	[Q10	D8]
23	$3d^5(^2I)4s$	^3I	0.7276	0.7526	[Q10	D8]
24	$3d^5(^6S)4p$	$^7P^o$	0.7516	0.7338	[O2	S6]
25	$3d^6$	^1D		0.7650	[	D8]
26	$3d^5(^2D3)4s$	^3D	0.7510	0.8126	[Q11	D9]
27	$3d^5(^4F3)4s$	^5F	0.7585	0.8038	[S6	Q11]
28	$3d^5(^2I)4s$	^1I	0.7603	0.8005	[	D9]
29	$3d^5(^2F2)4s$	^3F	0.7689	0.8211	[Q11	D9]
30	$3d^5(^2D3)4s$	^1D	0.7914	0.8601	[	D10]
31	$3d^5(^2F2)4s$	^1F	0.8010	0.8693	[	D10]
32	$3d^5(^2H)4s$	^3H	0.8090	0.8524	[Q12	D10]
33	$3d^5(^6S)4p$	$^5P^o$	0.8133	0.8295	[S7	Q12]
34	$3d^5(^2G2)4s$	^3G	0.8184	0.8679	[Q13	D10]
35	$3d^5(^4F)4s$	^3F	0.8244	0.8991	[Q13	D11]
36	$3d^5(^2H)4s$	^1H	0.8431	0.9000	[	D11]
37	$3d^5(^2F1)4s$	^3F	0.8511	0.9106	[Q13	D11]
38	$3d^5(^2G2)4s$	^1G	0.8521	0.9168	[	D11]
39	$3d^5(^2F1)4s$	^1F	0.8843	0.9582	[	D12]
40	$3d^6$	^1S		0.9596	[	D12]
41	$3d^5(^2S)4s$	^3S	0.8991	0.9721	[Q14	D12]
42	$3d^5(^2D2)4s$	^3D	0.9652	1.0406	[Q15	D13]
43	$3d^5(^2D2)4s$	^1D	0.9985	1.0908	[	D13]
44	$3d^5(^4G)4p$	$^5G^o$	1.0358	1.0353	[S8	Q15]
45	$3d^5(^2S)4s$	^1S		1.0310	[	D13]
46	$3d^5(^2G1)4s$	^3G	1.0419	1.1137	[Q16	D14]
47	$3d^5(^4G)4p$	$^5H^o$	1.0512	1.0507	[S9	Q16]

Table 1. (continued)

	State		Energy Obs.	Calc.	Target states	
48	$3d^5(^4G)4p$	$^5F^o$	1.0619	1.0717	[S9	Q16]
49	$3d^5(^4P)4p$	$^5S^o$	1.0653	1.0846	[S9	Q16]
50	$3d^5(^4P)4p$	$^5D^o$	1.0661	1.0825	[S9	Q16]
51	$3d^5(^2G1)4s$	^1G	1.0748	1.1619	[	D14]
52	$3d^5(^4G)4p$	$^3F^o$	1.0778	1.0965	[Q16	D14]
53	$3d^5(^4G)4p$	$^3H^o$	1.0800	1.0963	[Q16	D14]
54	$3d^5(^4P)4p$	$^5P^o$	1.0810	1.1083	[S9	Q16]
55	$3d^5(^4P)4p$	$^3P^o$	1.0921	1.1257	[Q17	D14]
56	$3d^5(^4D)4p$	$^5F^o$	1.1041	1.1220	[S10	Q17]
57	$3d^5(^4G)4p$	$^3G^o$	1.1112	1.1475	[Q17	D14]
58	$3d^5(^4P)4p$	$^3D^o$	1.1167	1.1567	[Q17	D14]
59	$3d^5(^4D)4p$	$^5D^o$	1.1208	1.1449	[S10	Q17]
60	$3d^5(^4D)4p$	$^5P^o$	1.1272	1.1509	[S10	Q17]
61	$3d^5(^4D)4p$	$^3D^o$	1.1381	1.1721	[Q18	D15]
62	$3d^5(^4D)4p$	$^3F^o$	1.1442	1.1784	[Q18	D15]
63	$3d^5(^4P)4p$	$^3S^o$	1.1518	1.2158	[Q18	D15]
64	$3d^5(^4D)4p$	$^3P^o$	1.1733	1.2231	[Q18	D15]
65	$3d^5(^2I)4p$	$^3K^o$	1.1873	1.1884	[Q18	D15]
66	$3d^5(^2I)4p$	$^3I^o$	1.1912	1.1932	[Q18	D15]
67	$3d^5(^2I)4p$	$^1H^o$	1.2002	1.2104	[	D15]
68	$3d^5(^2I)4p$	$^1K^o$	1.2028	1.2102	[	D15]
69	$3d^5(^2D)4p$	$^3F^o$	1.2064	1.2815	[Q18	D15]
70	$3d^5(^2I)4p$	$^3H^o$	1.2072	1.2223	[Q18	D15]
71	$3d^5(^2D)4p$	$^1D^o$	1.1978	1.2375	[	D15]
72	$3d^5(^2D)4p$	$^3P^o$	1.2252	1.2698	[Q18	D15]
73	$3d^5(^2F)4p$	$^1G^o$	1.2244	1.2554	[	D15]
74	$3d^5(^2F)4p$	$^3G^o$	1.2320	1.2635	[Q18	D15]
75	$3d^5(^4F)4p$	$^5G^o$	1.2339	1.2602	[S11	Q18]
76	$3d^5(^2D)4p$	$^3D^o$	1.2313	1.2790	[Q18	D15]
77	$3d^5(a^2F)4p$	$^3D^o$	1.2413	1.2859	[Q18	D15]
78	$3d^5(^2I)4p$	$^1I^o$	1.2369	1.2618	[	D15]
79	$3d^5(^2D)4p$	$^1F^o$	1.2411	1.2741	[	D15]
80	$3d^5(^4F)4p$	$^5F^o$	1.2402	1.2716	[S11	Q18]
81	$3d^5(a^2F)4p$	$^3F^o$	1.2453	1.2347	[Q18	D15]
82	$3d^5(^4F)4p$	^5D_o	1.2520	1.2847	[S11	Q18]
83	$3d^5(^2H)4p$	$^3H^o$	1.2566	1.2781	[Q18	D15]

Fe III configurations:
Spectroscopic: $1s^22s^22p^63s^23p^63d^6$, $1s^22s^22p^63s^23p^63d^54s$, $1s^22s^22p^63s^23p^63d^54p$
Correlation: $1s^22s^22p^63s^23p^43d^8$, $1s^22s^22p^63p^63d^8$, $1s^22s^22p^63s3p^63d^7$, $1s^22s^22p^63s3p^53d^8$, $1s^22s^22p^63s^23p^63d^54d$
λ_{nl}: 1.1 (1s), 1.1 (2s), 1.1 (2p), 1.095 (3s), 1.091 (3p), 1.0341 (3d), 1.04351 (4s), 1.044 66 (4p), 1.278 65 ($\overline{4d}$)

as degenerate in the present radiative calculations. We expect little consequent loss of accuracy since most of these states lie fairly high in energy. In table 1, the number of such terms that are treated degenerate is given next to the notation O, S, Q and D, mentioned earlier.

Following the R-matrix calculations for the e + Fe III system, we first obtain the energy levels of Fe II for all $SL\pi$ symmetries considered. For complex atoms and ions isoelectronic with the third and the fourth row elements, it is a non-trivial task to identify all the computed levels and a careful analysis is required based partly on a study of quantum defects along overlapping Rydberg series, and partly on the contributions of the closed channel wavefunctions, in the region outside the R-matrix boundary, to the total bound state. Nearly all Fe II states have been unambiguously identified. It might be noted that for the calculation of opacities the level identification problem is not consequential. However, we strive to attain precise LS term designations in order to facilitate other applications of the present data, particularly in the important extension of the OP work to obtain f-values for fine structure components within LS multiplets.

The work on Fe II was carried out on the 8 processor 64 MW Cray Y-MP at the Ohio Supercomputer Center, Columbus, Ohio. Table 2 shows the total CPU time required for the radiative calculations for octet, sextet, quartet and doublet symmetries, and the maximum memory needed for the R-matrix close coupling calculations with 83 state expansion for Fe II. It required up to 20 MW of memory for the largest $SL\pi$s and a total of about 450 CPU hours. Work was divided according to different symmetries, and the table shows the number of target states coupled to each $SL\pi$ and used as the target set of eigenfunctions for radiative calculations for that particular symmetry. For the largest of the quartet and doublet symmetries, the R-matrix calculations could be carried out for only one $SL\pi$ at a time.

Table 2. Summary of the radiative calculations for Fe II : N_{CC} is the number of target states coupled to a particular spin symmetry of Fe II, CPU is the amount of time required for that symmetry. Maximum memory requirement and disk space for a typical quartet or doublet symmetry run are given below. $N_{SL\pi}$ is the total number of bound symmetries, $SL\pi$ shows the range of these symmetries and N_{E_T} is the corresponding number of bound states up to $n \leqslant 10$, $l \leqslant 7$. N_{bnd} is the number of bound states below the first ionization threshold. N_f is the number of oscillator strengths. The largest case is $SL\pi = {}^2G$ with 181 continuum channels and the hamiltonian matrix size of 2228. Memory and disk space range requirements: RAM: 20 MW, disk: 3.5–4 GB.

Symmetry	N_{CC}	CPU	$N_{SL\pi}$	$SL\pi$ (range)	N_{E_T}	N_{bnd}	N_f
Octets	2	1.2 min	16	^{8}S–^{8}L, ^{8}S^o–^{8}K^o	92	6	95
Sextets	21	4.2 h	25	^{6}S–^{6}N, ^{6}S^o–^{6}O^o	234	205	4 267
Quartets	58	166.5 h	29	^{4}S–^{4}T, ^{4}S^o–^{4}R^o	357	308	9 965
Doublets	62	174.6 h	20	^{2}S–^{2}M, ^{2}S^o–^{2}M^o	618	224	21 614
Total	83	446 h†	90		1301	743	35 941

† Including about 100 CPU h spent on trials and problems

4. Results and discussions

Three sets of data are calculated: (a) energy levels, (b) oscillator strengths and (c) photoionization cross sections; these are discussed below with selected examples.

4.1. Energy levels

We obtain 1301 LS bound state and identify 743 states that lie below the first ionization threshold of Fe II, i.e. below the 3d^6(^{5}D) ground state of Fe III. In addition, a few bound states are obtained that lie above the ionization threshold but are forbidden to autoionize in LS coupling. The number of bound states that have been identified are more than twice the number that have been reportedly observed. Table 2 gives a summary of the number of bound state symmetries $SL\pi$, their total L and S value ranges, and the corresponding number of bound states computed for each $SL\pi$. All of the observed LS terms, 266 in total, have been calculated and identified. This could not have been possible with the earlier 16-CC R-matrix calculations (Sawey and Berrington 1992) because several of the observed states couple to terms dominated by excited configurations $3d^5 4s$ and $3d^5 4p$ of Fe III which are not included in the earlier work. The present calculated energy for the $3d^6 4s(^6D)$ ground state of Fe II differs by 0.6% from the observed value, compared to a 7% discrepancy in the previous calculation.

In table 3 we compare the calculated and observed energies. The latter set includes recent measurements from the Lund group (Johansson 1992); the LS energies have been computed as the statistically weighted average over the fine structure components. In a small number of cases the set of observed fine structure levels is incomplete; such states are marked with asterisks. Comparison shows that most of the calculated LS term energies are within 10% of the observed ones, yet many do show larger differences of up to 10–30%. Exclusion of relativistic effects is probably the prime contributor to the discrepancies. While the relativistic calculations are planned, as part of a new project on the iron-peak elements (the Iron Project), using Breit–Pauli R-matrix method, it is estimated that the *ab initio* fine structure calculations may require an order of magnitude more resources and effort even over the present one.

4.2. *Oscillator strengths*

Dipole oscillator strengths (f-values) for approximately 36 000 transitions among the 1301 calculated bound states of Fe II are obtained in LS coupling. Over 19 000 of these transitions are between bound states which lie below the first ionization threshold. For opacity calculations we also include transitions of bound states when the lower state lies below the first ionization threshold and the upper state lies above; since the latter do not appear as resonances in the photoionization cross sections in LS coupling but the corresponding oscillator strength does contribute to total photoabsorption. Table 2 lists the number of oscillator strengths obtained for each spin symmetry and all corresponding total angular momenta L. Each oscillator strength in LS coupling corresponds to a number of transitions, when we consider the fine structure, resulting in over 100 000 individual f-values. These calculations are discussed below.

As an enormous amount of data have been computed, one of the primary aims of this report is to attempt to establish the uncertainties involved relative to available experimental data and previous theoretical calculations. Table 4(a) presents selected comparisons with other results found in literature. The present oscillator strengths are obtained from the calculated line strength (s), and the observed energies, according to the relation, $S=(3g_i/E_{fi})f_{if}$. Of the two sets of columns for transition of states in the table, the first set of columns compares the present results with both the measured values compiled by NIST (Fuhr *et al* 1988) and the calculated ones by Kurucz (1981), and the second set of columns with those of Kurucz. NIST has compiled and evaluated all the available measured and some theoretical values for the oscillator strengths. The column listing the NIST f-values for dipole allowed transitions in LS coupling are averaged over the fine structure transitions for most cases. Kurucz obtained the f-values using semi-empirical atomic structure calculations including some relativistic effects (his f-values quoted in table 4(a) are statistically averaged over the fine structure).

For most cases the present values agree within 10% with those by Kurucz. Overall we find that the present LS multiplet oscillator strengths are in somewhat better agreement with the experimental values than those of Kurucz for most transitions (this is

Table 3. Comparison of calculated (cal) energies (in Ry) of the octet, sextet, quartet and doublet states of Fe II with the observed (obs) ones. * denotes that the observed *LS* energy is obtained from incomplete set of fine structure levels The table contains the most recent measured values of the energy levels at Lund (Johansson 1992).

State		E (Ry) Obs.	E (Ry) Calc.	State		E (Ry) Obs.	E (Ry) Calc.
			Octets: 2-cc				
$3d^5\,^6S4s4p\,^3P^o$	z^8P^o	0.709 72	0.7783	$3d^54s\,^7S\,5s$	^8S	0.250 23	0.2457
$3d^54p^2$	^8P	0.215 67	0.2742	$3d^54s\,^7S\,4d$	^8D	0.192 13	0.2300
			Sextets: 21-cc				
$3d^6\,^5D4s$	a^6D	1.185 91	1.1782	$3d^5\,^4D4s4p$	$^6D^o$	0.333 45	0.3478
$3d^54s^2$	a^6S	0.977 21	0.9951	$3d^5\,^4D4s4p$	$^6P^o$	0.327 51	0.3443
$3d^5\,^5D4p$	z^6D^o	0.836 95	0.8466	$3d^5\,^5D6s$	^6D	0.259 37	0.2555
$3d^5\,^5D4p$	z^6F^o	0.805 42	0.8177	$3d^5\,^5D5d$	^6F	0.240 42*	0.2454
$3d^5\,^5D4p$	z^6P^o	0.797 26	0.8111	$3d^5\,^5D5d$	^6P	0.239 87	0.2438
$3d^5\,^6S4s4p$	y^6P^o	0.623 92	0.6594	$3d^5\,^5D5d$	^6D	0.236 33	0.2422
$3d^5\,^6S4s4p$	x^6P^o	0.467 09	0.4785	$3d^5\,^5D5d$	^6G	0.234 92	0.2417
$3d^5\,^5D5s$	e^6D	0.476 40	0.4687	$3d^5\,^5D5d$	^6S	0.226 38	0.2388
$3d^5\,^5D4d$	e^6F	0.423 50	0.4312	$3d^54p^2$	^6D	0.218 62	0.2713
$3d^5\,^5D4d$	^6D	0.426 04	0.4273	$3d^54s\,^7S5s$	^6S	0.218 35	0.2117
$3d^5\,^5D4d$	^6P	0.421 30	0.4219	$3d^5\,^4F4s4p$	$^6F^o$	0.218 56	0.2275
$3d^5\,^5D4d$	e^6G	0.420 21	0.4223	$3d^5\,^5D6p$	$^6D^o$	0.217 65	0.2197
$3d^5\,^5D4d$	^6S	0.410 61	0.4128	$3d^5\,^5D6p$	$^6F^o$	0.212 07	0.2146
$3d^5\,^4G4s4p$	y^6F^o	0.392 40	0.3756	$3d^5\,^5D6p$	$^6P^o$	0.210 58	0.2126
$3d^5\,^4P4s4p$	^6D_o	0.385 57	0.4120	$3d^5\,^4F4s4p$	$^6D^o$	0.204 51	0.2116
$3d^5\,^5D5p$	$^6D^o$	0.378 96	0.3789	$3d^5\,^5D7s$	^6D	0.162 27	0.1638
$3d^5\,^4P4s4p$	$^6P^o$	0.375 53	0.3966	$3d^5\,^5D6d$	^6F	0.153 54*	0.1568
$3d^5\,^5D5p$	$^6F^o$	0.367 66	0.3675	$3d^5\,^5D6d$	^6G	0.151 48*	0.1550
$3d^5\,^5D5p$	$^6P^o$	0.356 31	0.3581	$3d^54p^2$	^6P	0.141 66	0.1834
$3d^5\,^4D4s4p$	$^6F^o$	0.349 40	0.3756	$3d^54s\,^7S4d$	^6D	0.129 55	0.1446
			Quartets: 58-cc				
$3d^7$	a^4F	1.167 68	1.081	$3d^54s\,^3I4p$	$^4K^o$	0.254 88	0.2852
$3d^6\,^5D4s$	a^4D	1.113 88	1.1060	$3d^6\,^5D6s$	^4D	0.253 38	0.2531
$3d^7$	a^4P	1.065 66	0.9846	$3d^6\,^3G5s$	f^4G	0.252 41	0.2403
$3d^6\,^3P4s$	b^4P	0.994 50	0.9313	$3d^54s\,^3I4p$	$^4I^o$	0.250 27	0.2810
$3d^6\,^3H4s$	a^4H	0.994 15	0.9631	$3d^6\,^3P4d$	^4D	0.249 70*	0.2206
$3d^6\,^3F4s$	b^4F	0.981 86	0.9327	$3d^6\,^3H4d$	^4K	0.244 07*	0.2120
$3d^6\,^3G4s$	a^4G	0.954 95	0.9168	$3d^6\,^3H4d$	^4H	0.243 99	0.2104
$3d^6\,^3D4s$	b^4D	0.903 38	0.8499	$3d^6\,^3H4d$	^4G	0.243 87	0.2112
$3d^6\,^5D4p$	z^4F^o	0.782 23	0.7968	$3d^6\,^5D5d$	^4F	0.243 20	0.2377
$3d^6\,^5D4p$	z^4D^o	0.781 97	0.7890	$3d^6\,^3P4d$	^4F	0.242 56	0.2188
$3d^6\,^5D4p$	z^4P^o	0.759 42	0.7706	$3d^6\,^3H4d$	^4I	0.241 46	0.2106
$3d^6\,^3P4s$	c^4P	0.735 96	0.6515	$3d^6\,^3P4d$	^4P	0.234 41	0.2206
$3d^6\,^3F4s$	c^4F	0.732 69	0.6462	$3d^54s\,^3I4p$	$^4H^o$	0.234 39	0.2606
$3d^54s^2$	b^4G	0.695 23	0.6913	$3d^54s\,^3D4p$	$^4F^o$	0.233 14	0.2367
$3d^54s^2$	d^4P	0.666 03	0.6331	$3d^6\,^5D5d$	^4D	0.232 53*	0.2404
$3d^6\,^3P4p$	z^4S^o	0.646 01	0.6075	$3d^6\,^3H4d$	^4F	0.232 40*	0.2007
$3d^64s^2$	c^4D	0.639 58	0.6191	$3d^6\,^3F4d$	^4D	0.231 06*	0.1940
$3d^6\,^3P4p$	y^4P^o	0.635 49	0.5997	$a3d^6\,^3F4d$	^4G	0.231 07	0.1946
$3d^6\,^3F4p$	y^4F^o	0.623 42	0.5947	$3d^6\,^5D5d$	^4G	0.230 88	0.2389
$3d^6\,^3H4p$	z^4G^o	0.635 48	0.6168	$3d^6\,^3Fa4d$	^4H	0.228 98	0.1939
$3d^6\,^3H4p$	z^4H^o	0.634 34	0.6193	$3d^6\,^3F4d$	^4F	0.216 64	0.1875
$3d^6\,^3H4p$	z^4I^o	0.629 42	0.6194	$3d^6\,^5D5d$	^4P	0.215 10	0.2267
$3d^6\,^3P4p$	y^4D^o	0.621 32	0.5896	$3d^54s\,^3D4p$	$^4D^o$	0.213 54	0.2129
$3d^6\,^3F4p$	x^4D^o	0.613 70	0.5857	$3d^54s\,^3D4p$	$^4P^o$	0.219 16*	0.2129
$3d^6\,^3F4p$	y^4G^o	0.606 78	0.5844	$3d^6\,^3F4d$	^4F	0.216 61	0.1875

Table 3. (continued)

State		E (Ry) Obs.	Calc.	State		E (Ry) Obs.	Calc.
$3d^6\,^3G4p$	x^4G^o	0.590 33	0.5723	$3d^6\,^5D6p$	$^4D^o$	0.213 08*	0.2101
$3d^6\,^3G4p$	x^4F^o	0.585 42	0.5645	$3d^6\,^5D6p$	$^4F^o$	0.212 78	0.2133
$3d^6\,^3G4p$	y^4H^o	0.583 58	0.5669	$3d^6\,^5D6p$	$^4P^o$	0.209 37	0.2101
$3d^5\,4s^5S4p$	x^4P^o	0.558 89	0.5729	$3d^54s^3F4p$	$^4G^o$	0.208 68*	0.2115
$3d^6\,^3D4p$	w^4P^o	0.533 29	0.5009	$3d^54s^3F4p$	$^4D^o$	0.202 48*	0.1984
$3d^6\,^3D4p$	w^4F^o	0.529 87	0.5007	$3d^6\,^3P5p$	$^4S^o$	0.202 14	0.1919
$3d^6\,^3D4p$	w^4D^o	0.528 17	0.4962	$3d^6\,^3G4d$	^4G	0.201 97	0.1830
$3d^54s^2$	^4F	0.520 31	0.4884	$3d^6\,^3G4d$	^4H	0.201 81	0.1830
$3d^6\,^5D5s$	e^4D	0.462 40	0.4555	$3d^54s^3F4p$	$^4F^o$	0.201 41	0.2022
$3d^6\,^5D4d$	f^4D	0.416 38	0.4225	$3d^54s^3G4p$	$^4G^o$	0.200 38	0.1948
$3d^6\,^5D4d$	e^4G	0.413 10	0.4195	$3d^6\,^3G4d$	^4I	0.200 19	0.1812
$3d^6\,^5D4d$	^4S	0.408 48	0.4142	$3d^6\,^3G4d$	^4D	0.200 03	0.1808
$3d^6\,^5D4d$	e^4F	0.402 42	0.3933	$3d^6\,^3D5s$	^4D	0.198 84	0.1860
$3d^6\,^3P4p$	v^4D^o	0.399 18	0.3401	$3d^564s^3G4p$	$^4H^o$	0.198 10	0.2010
$3d^6\,^5D4d$	^4P	0.387 09	0.3747	$3d^6\,^3P5p$	$^4P^o$	0.195 11	0.1868
$b3d^6\,^3F4p$	$^4G^o$	0.369 44	0.3475	$3d^6\,^3H5p$	$^4I^o$	0.190 04	0.1751
$3d^6\,^3P4p$	$^4S^o$	0.363 82	0.3144	$3d^6\,^3H5p$	$^4G^o$	0.188 33	0.1588
$3d^6\,^5D5p$	$^4D^o$	0.363 36	0.3631	$3d^6\,^3P5p$	$^4D^o$	0.187 67*	0.1802
$3d^6\,^5D5p$	$^4F^o$	0.362 61	0.3654	$3d^6\,^3G4d$	^4F	0.185 85	0.1695
$3d^6\,^5D5p$	$^4P^o$	0.355 18	0.3575	$3d^6\,^3F5p$	$^4F^o$	0.185 29	0.1664
$3d^6\,^3P4p$	$^4P^o$	0.355 19	0.3348	$3d^54s^3G4p$	$^4H^o$	0.184 13*	0.1380
$3d^54s^5G4p$	x^4H^o	0.349 80	0.3693	$3d^6\,^4F5p$	$^4D^o$	0.182 37*	0.1537
$3d^54s^5G4p$	v^4F^o	0.348 10	0.3618	$3d^6\,^3H5p$	$^4H^o$	0.172 27	0.1821
$3d^6\,^3F4p$	$^4D^o$	0.343 16	0.3100	$3d^6\,^3F5p$	$^4G^o$	0.169 26	0.1498
$3d^6\,^3F4p$	u^4F^o	0.338 17	0.2981	$3d^54s^3H4p$	$^4I^o$	0.167 56*	0.1444
$3d^54s^5G4p$	w^4G^o	0.332 03	0.3085	$3d^6\,^3G5p$	$^4F^o$	0.166 97	0.1575
$3d^54s^5P4p$	$^4P^o$	0.328 56	0.2877	$3d^54s^5F4p$	$^4G^o$	0.165 94*	0.1777
$3d^54s^5P4p$	$^4D^o$	0.314 57	0.2952	$3d^6\,^5D7s$	^4D	0.158 33	0.1614
$3d^6\,^3P5s$	^4P	0.296 95	0.2832	$3d^6\,^5D6d$	^4F	0.149 40*	0.1396
$3d^6\,^3H5s$	e^4H	0.293 68	0.2404	$3d^6\,^3G5p$	$^4H^o$	0.148 92*	0.1455
$3d^54s^5P4p$	$^4S^o$	0.293 58	0.2718	$3d^6\,^5D6d$	^4G	0.146 62	0.1538
$3d^54s^5D4p$	$^4F^o$	0.292 37	0.2822	$3d^6\,^3G5p$	$^4G^o$	0.142 92*	0.1402
$3d^54s^5D4p$	$^4D^o$	0.291 53	0.2782	$3d^6\,^3D4d$	^4F	0.141 46*	0.1158
$3d^6\,^3F5s$	f^4F	0.218 08	0.2401	$3d^54p^2$	^4P	0.112 86*	0.1231
$3d^54s^5D4p$	$^4P^o$	0.263 75	0.2558				
			Doublets: 62-CC				
$3d^7$	a^2G	1.043 19	0.9380	$3d^6b^3P4p$	u^2D^o	0.346 74	0.2851
$3d^7$	a^2P	1.020 79	0.9148	$3d^6b^3F4p$	$^2D^o$	0.326 72*	0.2698
$3d^7$	a^2H	1.002 42	0.9222	$3d^6b^3P4p$	$^2P^o$	0.323 64*	0.2902
$3d^7$	a^2D	0.999 85	0.8896	$3d^6b^3F4p$	$^2F^o$	0.323 40	0.3180
$3d^6a^3P4s$	b^2P	0.951 23	0.8763	$3d^54s^3G4p$	$^2H^o$	0.313 58	0.3181
$3d^6\,^3H4s$	b^2H	0.950 46	0.8958	$3d^54s^3G4p$	$^2F^o$	0.311 93	0.2582
$3d^6a^3F4s$	a^2F	0.939 60	0.8905	$3d^54s^3P4p$	$^2P^o$	0.302 80*	0.2533
$3d^6\,^3G4s$	b^2G	0.911 26	0.8667	$3d^6b^1G4p$	$^2H^o$	0.295 89	0.2394
$3d^7$	b^2F	0.898 83	0.7842	$3d^6b^1G4p$	$^2F^o$	0.288 47*	0.2350
$3d^6\,^1I4s$	a^2I	0.889 97	0.8470	$3d^6\,^3H5s$	e^2H	0.285 71	0.2324
$3d^6a^1G4s$	c^2G	0.884 59	0.8307	$3d^6\,^3P5s$	^2P	0.284 33	0.2750
$3d^6\,^3D4s$	b^2D	0.859 80	0.7966	$3d^54s^3G4p$	$^2G^o$	0.281 66	0.2741
$3d^6a^1S4s$	a^2S	0.850 46	0.7887	$3d^6b^1G4p$	$^2G^o$	0.280 44	0.2090
$3d^6a^1D4s$	c^2d	0.841 74	0.7565	$3d^54s^3P4p$	$^2D^o$	0.274 78*	0.2521
$3d^6\,^1F4s$	c^2F	0.780 35	0.6907	$3d^6a^3F5s$	e^2F	0.272 94	0.2314
$3d^7$	d^2D	0.753 26	0.6128	$3d^54s^3D4p$	$^2D^o$	0.255 92	0.2379
$3d^6b^3P4s$	c^2P	0.691 94	0.5975	$3d^54s^3D4p$	$^2F^o$	0.248 83	0.2101
$3d^6b^3F4s$	d^2F	0.689 51	0.5997	$3d^6\,^3G5s$	e^2G	0.244 03	0.2310

Table 3. (continued)

State		E (Ry) Obs.	E (Ry) Calc.	State		E (Ry) Obs.	E (Ry) Calc.
$3d^6b^1G4s$	d^2G	0.655 27	0.5513	$3d^54s^3P4p$	$^2S^o$	0.242 28	0.2123
$3d^6a^3P4p$	z^2D^o	0.629 21	0.5944	$3d^6\,^3H4d$	^2K	0.240 06	0.2092
$3d^6\,^3H4p$	z^2G^o	0.622 99	0.6072	$3d^6\,^3H4d$	^2F	0.238 66	0.2066
$3d^6\,^3H4p$	z^2I^o	0.620 49	0.5575	$3d^6\,^3H4d$	^2G	0.233 35	0.2008
$3d^6a^3F4p$	z^2F^o	0.603 34	0.5794	$3d^6\,^3H4d$	^2I	0.235 71	0.2061
$3d^6a^3P4p$	z^2P^o	0.598 97	0.5633	$3d^6\,^3P4d$	^2P	0.231 74	0.2095
$3d^6a^3F4p$	y^2G^o	0.597 78	0.5713	$3d^6\,^3P4d$	^2D	0.230 69*	0.2108
$3d^6\,^3H4p$	z^2H^o	0.593 26	0.5772	$3d^6a^3F4d$	^2H	0.224 86	0.1917
$3d^6a^3P4p$	z^2S^o	0.586 00	0.5491	$3d^6\,^3H4d$	^2H	0.223 13	0.1896
$3d^6a^3F4p$	y^2D^o	0.578 15	0.5498	$3d^6a^3F4d$	^2F	0.221 86*	0.1920
$3d^6\,^3G4p$	y^2H^o	0.572 44	0.5581	$3d^54s^3D4p$	$^2P^o$	0.220 47	0.2001
$3d^6\,^3G4p$	y^2F^o	0.555 23	0.5278	$3d^64s^3I4p$	$^2K^o$	0.220 43	0.2409
$3d^6\,^3G4p$	x^2G^o	0.548 10	0.5262	$3d^64s^3I4p$	$^2H^o$	0.216 16	0.2158
$3d^6\,^1I4p$	z^2K^o	0.540 65	0.5211	$3d^6a^3F4d$	^2G	0.215 43	0.1849
$3d^6a^1G4p$	x^2H^o	0.531 75	0.5012	$3d^6a^3F4d$	^2D	0.210 85	0.1754
$3d^6a^1G4p$	x^2F^o	0.524 18	0.4907	$3d^6a^3F4d$	^2P	0.204 57*	0.1648
$3d^6a^1G4p$	w^2G^o	0.523 43	0.4883	$3d^6\,^1I5s$	^2I	0.199 70	0.1374
$3d^6\,^3D4p$	y^2P^o	0.522 76	0.4852	$3d^6\,^3P5p$	$^2D^o$	0.197 03*	0.1840
$3d^6\,^1I4p$	w^2H^o	0.518 36	0.4880	$3d^6\,^3G4d$	^2I	0.194 54	0.1786
$3d^6\,^1I4p$	y^2I^o	0.515 65	0.4927	$3d^54s^3I4p$	$^2I^o$	0.194 54	0.2054
$3d^6\,^3D4p$	x^2D^o	0.510 23	0.4747	$3d^6\,^3D5s$	^2D	0.190 66	0.1316
$3d^6\,^3D4p$	w^2F^o	0.499 55	0.4606	$3d^6\,^3G4d$	^2G	0.189 60	0.1638
$3d^6a^1S4p$	x^2P^o	0.494 60	0.4429	$3d^6\,^3G4d$	^2H	0.188 85	0.1625
$3d^54s^2$	^2H	0.485 92*	0.4588	$3d^6\,^3H5p$	$^2G^o$	0.185 30	0.1452
$3d^6a^1D4p$	v^2F^o	0.479 20	0.4212	$3d^6\,^3G4d$	^2D	0.185 26	0.1646
$3d^54s^2$	^2G	0.475 24	0.4459	$3d^6\,^3H5p$	$^2I^o$	0.186 64	0.1231
$3d^6a^1D4p$	w^2D^o	0.473 36	0.4134	$3d^6\,^3G4d$	^2F	0.181 95	0.1519
$3d^6a^1D4p$	w^2P^o	0.468 80	0.4130	$3d^54s^3F4p$	$^2G^o$	0.181 28*	0.1823
$3d^54s^2$	^2F	0.445 25	0.4881	$3d^6\,^3H5p$	$^2H^o$	0.180 07	0.1370
$3d^6\,^1F4p$	v^2G^o	0.427 70	0.3710	$3d^6\,^3F5p$	$^2G^o$	0.172 93	0.1399
$3d^6\,^1F4p$	v^2D^o	0.423 64	0.3630	$3d^6\,^3F5p$	$^2F^o$	0.171 92	0.1417
$3d^6\,^1F4p$	u^2F^o	0.401 36	0.3411	$3d^6\,^3G5p$	$^2H^o$	0.145 10	0.1415
$3d^6b^3P4p$	$^2S^o$	0.378 64	0.3210	$3d^6\,^3G5p$	$^2G^o$	0.142 85*	0.1310
$3d^6b^3F4p$	u^2G^o	0.348 02	0.2886				

also true of the fine structure f-values discussed in the next section). The comparison needs to be viewed in light of the following: while the present calculations do not explicitly account for the relativistic effects, some allowance is made by using observed energies to obtain the f-values with improved accuracy. The electron correlation effects should be better represented in the present work, based on *ab initio* close coupling calculations, than the semi-empirical method of Kurucz involving fitting of parameters to observed energy levels. For most transitions therefore the present data for Fe II obtained in this manner should be at least as accurate as currently available values. The present results provide an alternative dataset for a large number of oscillator strengths for Fe II, although it is difficult to state the uncertainties precisely. The *LS* coupling f-values given in table 4(a) provide an overall indication of the accuracy of the total multiplet strengths in the total dataset.

In table 4(b) we further extend the comparisons to the fine structure components, obtained through algebraic transformation (Allen 1976) as described earlier. Only

Table 4. (*a*) Comparison of oscillator strengths, f_{if}, of Fe II in *LS* coupling. ΔE is the transition energy. (*b*) Comparison of fine structure oscillator strengths for transitions in Fe II. For each transition the first line corresponds to the *LS* values and the following lines to the fine structure components. (*c*) Calculated and measured lifetimes, τ, of Fe II levels.

(*a*)

Transition	ΔE (Ry)	f_{if} Present	f_{if} NIST	f_{if} Kurucz	Transition	ΔE (Ry)	f_{if} Present	f_{if} Kurucz
$a\,^6S \to z\,^6P^o$	0.180	0.0434	0.041	0.0196	$a\,^6D \to z\,^6P^o$	0.389	0.126	0.094
$a\,^6D \to z\,^6D^o$	0.350	0.2945	0.26	0.297	$a\,^6D \to z\,^6F^o$	0.382	0.399	0.413
$a\,^4P \to z\,^4P^o$	0.306	0.0838	0.066	0.106	$z\,^6P^o \to e\,^6D$	0.321	0.142	0.149
$a\,^4P \to z\,^4D^o$	0.284	0.0273	0.0168	0.0289	$b\,^4P \to y\,^4P^o$	0.359	0.210	0.263
$b\,^4P \to z\,^4D^o$	0.213	8.0 (−5)	0.0028	0.0029	$a\,^4D \to z\,^4D^o$	0.332	0.281	0.273
$a\,^4D \to z\,^4P^o$	0.354	0.142	0.13	0.152	$b\,^4D \to z\,^4P^o$	0.144	1.12 (−3)	1.10 (−3)
$a\,^4D \to z\,^4F^o$	0.332	0.378	0.33	0.351	$b\,^4D \to z\,^4D^o$	0.121	4.2 (−4)	4.5 (−4)
$a\,^4F \to z\,^4F^o$	0.385	0.0431	0.031	0.050	$a\,^4F \to z\,^4D^o$	0.386	0.085	0.0804
$b\,^4F \to z\,^4F^o$	0.200	8.7 (−4)	7.1 (−4)	8.6 (−4)	$a\,^4H \to z\,^4H^o$	0.360	0.243	0.255
$a\,^2S \to z\,^2P^o$	0.251	0.0132	0.0084	0.023	$a\,^4H \to z\,^4G^o$	0.359	0.170	0.132
$a\,^2S \to y\,^2P^o$	0.328	0.112	0.0087	0.265	$b\,^4P \to z\,^4S^o$	0.348	0.0663	0.0087
$a\,^2S \to x\,^2P^o$	0.356	0.535	0.39	0.536	$b\,^2D \to y\,^2P^o$	0.337	0.120	0.108
$b\,^2P \to z\,^2P^o$	0.352	0.208	0.23	0.26	$b\,^2D \to x\,^2D^o$	0.350	0.276	0.261
$c\,^2D \to x\,^2P^o$	0.347	0.0557	0.098	0.035	$a\,^2F \to y\,^2G^o$	0.342	0.337	0.280
$a\,^2F \to z\,^2F^o$	0.336	0.202	0.14	0.109	$c\,^2F \to v\,^2D^o$	0.357	0.182	0.168
$b\,^2F \to x\,^2G^o$	0.351	0.0661	0.042	0.0668	$d\,^2F \to u\,^2G^o$	0.341	0.223	0.183
$c\,^2F \to v\,^2G^o$	0.353	0.342	0.31	0.349	$b\,^2P \to z\,^2D^o$	0.322	0.106	0.217
$b\,^2G \to y\,^2F^o$	0.356	0.182	0.13	0.147	$b\,^2P \to z\,^2S^o$	0.365	0.0036	0.080
$b\,^2G \to y\,^2G^o$	0.313	1.0 (−4)	3.8 (−3)	3.8 (−3)	$b\,^2D \to z\,^2D^o$	0.231	1.3 (−3)	1.4 (−3)
$b\,^2G \to y\,^2H^o$	0.339	0.230	0.18	0.21	$b\,^2H \to z\,^2H^o$	0.357	0.161	0.0946
$c\,^2G \to z\,^2F^o$	0.281	9.1 (−3)	5.2 (−3)	6.0 (−3)	$b\,^2H \to z\,^2I^o$	0.330	0.158	0.278
$c\,^2G \to x\,^2H^o$	0.353	0.140	0.17	0.278	$a\,^2I \to z\,^2H^o$	0.297	0.119	0.110
$b\,^2H \to z\,^2G^o$	0.327	0.0122	0.069	0.108	$c\,^2G \to z\,^2G^o$	0.262	6.5 (−3)	6.7 (−3)

(*b*)

Transition	λ_{if} (Å)	g_i	g_f	f_{if} Present	f_{if} NIST	f_{if} Kurucz	λ_{if} (Å)	g_i	g_f	f_{if} Present	f_{if} NIST	f_{if} Kurucz
$a\,^6S^e \to z\,^6P^o$		6	18	0.0434	0.041	0.0196						
	5170	6	8	0.0189	0.023	0.0083	4925	6	4	0.0099	0.008	0.0046
	5020	6	6	0.0146	0.010	0.0066						
$a\,^6D^e \to z\,^6P^o$		30	18	0.126		0.0938						
	2344	10	8	0.126	0.11	0.129	2360	4	6	0.0377		0.0718
	2366	8	8	0.0449	0.051	0.0566	2328	6	4	0.0396	0.032	0.039
	2381	6	8	0.0099	0.036	0.0392	2339	4	4	0.0887	0.087	0.103
	2334	8	6	0.0814		0.0805	2345	2	4	0.126	0.13	0.177
	2349	6	6	0.077		0.094						
$a\,^6D^e \to z\,^6D^o$		30	30	0.294	0.26	0.297						
	2600	10	10	0.240	0.22	0.261	2608	6	4	0.118	0.11	0.133
	2587	10	8	0.0548	0.065	0.0766	2632	4	6	0.175	0.12	0.133
	2626	8	10	0.0675	0.043	0.0459	2621	4	4	0.00322	0.0037	0.003 95
	2613	8	8	0.131	0.11	0.135	2615	4	2	0.114	0.10	0.119
	2599	8	6	0.0948	0.099	0.117	2629	2	4	0.227	0.18	0.188
	2632	6	8	0.125	0.084	0.0887	2622	2	2	0.0652	0.050	0.0587
	2618	6	6	0.0502	0.045	0.0517						
$a\,D^e \to z\,^6F^o$		30	42	0.397		0.413						
	2383	10	12	0.342	0.328	0.36	2400	6	6	0.131	0.12	0.130
	2374	10	10	0.0527	0.028	0.0340	2396	6	4	0.0227	0.019	0.017
	2368	10	8	0.004 25		4.4 (−5)	2411	4	6	0.203	0.19	0.232
	2396	8	10	0.289	0.27	0.323	2407	4	4	0.161	0.14	0.167
	2389	8	8	0.0968	0.089	0.0924	2405	4	2	0.0314	0.031	0.0290
	2384	8	6	0.0122		0.0057	2414	2	4	0.175	0.19	0.200
	2406	6	8	0.243	0.20	0.265	2412	2	2	0.220	0.21	0.236
$a\,^4P^e \to z\,^4P^o$		12	12	0.0838	0.066	0.106						
	2986	6	6	0.0585	0.048	0.0763	2945	4	2	0.0353	0.03	0.0452
	2949	6	4	0.0254	0.017	0.0327	2986	2	4	0.0696	0.048	0.0843
	3004	4	6	0.0374	0.029	0.0427	2965	2	2	0.0140	0.012	0.0169
	2966	4	4	0.0112	0.0079	0.0154						
$a\,^4P^e \to z\,^4D^o$		12	20	0.0273	0.0168	0.0289						
	3229	6	8	0.0217	0.012	0.023	3188	4	4	0.00881	0.0049	0.008 34
	3194	6	6	0.00495	0.0019	0.003 36	3171	4	2	0.00139	6.9 (−4)	0.001 16

Table 4. (continued)

Transition	λ_{if} (Å)	g_i	g_f	f_{if} Present	f_{if} NIST	f_{if} Kurucz	λ_{if} (Å)	g_i	g_f	f_{if} Present	f_{if} NIST	f_{if} Kurucz
	3168	6	4	5.5 (−4)	1.4 (−4)	2.8 (−4)	3211	2	4	0.0137	0.0081	0.0170
	3214	4	6	0.0172	0.015	0.0206	3195	2	2	0.0137	0.0095	0.0153
$a\,^4D^e \to z\,^4P^o$		20	12	0.142	0.13	0.152						
	2563	8	6	0.143	0.11	0.144	2583	4	4	0.0754	0.077	0.0885
	2592	6	6	0.0423	0.052	0.055	2595	2	4	0.0235	0.026	0.0306
	2612	4	6	0.0070	0.0093	0.011	2568	4	2	0.0593	0.056	0.0604
	2564	6	4	0.0997	0.085	0.0995	2579	2	2	0.118	0.13	0.132
$a\,^4D^e \to z\,^4D^o$		20	20	0.281		0.273						
	2740	8	8	0.241	0.22	0.268	2770	4	6	0.0973	0.0077	0.0267
	2715	8	6	0.0404	0.045	0.05	2750	4	4	0.112	0.12	0.131
	2774	6	8	0.0528	8.0 (−5)	0.0049	2738	4	2	0.0703		0.0713
	2748	6	6	0.161	0.18	0.189	2763	2	4	0.139	0.026	0.0632
	2728	6	4	0.0659	0.063	0.0746	2750	2	2	0.140	0.12	0.131
$a\,^4D^e \to z\,^4F^o$		20	28	0.378	0.33	0.351						
	2757	8	10	0.336	0.30	0.266	2710	6	4	0.00365	1.9 (−4)	2.3 (−4)
	2718	8	8	0.0389	0.0011	0.0041	2747	4	6	0.303	0.33	0.364
	2694	8	6	0.00199	0.001	7.2 (−5)	2732	4	4	0.0760	0.028	0.0485
	2750	6	8	0.308	0.32	0.351	2744	2	4	0.378	0.41	0.446
	2726	6	6	0.0662	0.011	0.0264						
$b\,^4D^e \to x\,^4D^o$		20	20	0.0223		0.02						
	3178	8	8	0.0189	0.012	0.017	3134	4	6	0.00782	0.0035	0.0037
	3146	8	6	0.00317	0.0023	0.0032	3115	4	4	0.00899	0.0098	0.0099
	3169	6	8	0.0042		5.8 (−4)	3106	4	2	0.00564	0.0057	0.0058
	3136	6	6	0.0128	0.012	0.014	3116	2	4	0.0112	0.0081	0.0085
	3117	6	4	0.00524	0.0068	0.0058	3106	2	2	0.0113	0.011	0.0108
$a\,^4F^e \to z\,^4D^o$		28	20	0.0854		0.0804						
	2349	10	8	0.0859	0.034	0.0794	2400	4	6	0.00168		0.0041
	2380	8	8	0.0121	0.13	0.0257	2369	6	4	0.0639	0.033	0.0609
	2403	6	8	8.1 (−4)	0.0022	0.0028	2385	4	4	0.0237	0.020	0.036
	2361	8	6	0.0733	0.037	0.066	2376	4	2	0.0595	0.041	0.0648
	2384	6	6	0.0206	0.029	0.035						
$a\,^4F^e \to z\,^4F^o$		28	28	0.0431	0.031	0.050						
	2361	10	10	0.0396	0.020	0.0429	2386	6	8	0.00763	0.0038	0.006 57
	2332	10	8	0.00362	0.019	0.0206	2367	6	6	0.0296	0.0084	0.0191
	2392	8	10	0.00442	0.0029	0.00504	2356	6	4	0.00577	0.013	0.0150
	2363	8	8	0.0329	0.011	0.0227	2383	4	6	0.00856	0.0051	0.007 14
	2345	8	6	0.00583	0.018	0.0208	2371	4	4	0.0344	0.012	0.0265
$a\,^2S^e \to z\,^2P^o$		2	6	0.0132	0.0084	0.023						
	3622	2	4	0.00878	0.0051	0.015	3626	2	2	0.00438	0.0035	0.008
$a\,^2S^e \to y\,^2P^o$		2	6	0.113	0.0087	0.265						
	2781	2	4	0.0749	0.054	0.085	2781	2	2	0.0374	0.034	0.18
$a\,^2S^e \to x\,^2P^o$		2	6	0.535	0.39	0.536						
	2571	2	4	0.355	0.23	0.347	2541	2	2	0.180	0.15	0.188

(*c*)

State	J	τ (ns) Present	τ (ns) Expt	τ (ns) Kurucz
$z\,^6P^o$	7/2	3.884	3.73(0.06)[a], 3.8(0.2)[b] 3.5(0.3)[c], 3.73(0.05)[d]	3.28
$z\,^6P^o$	5/2	3.844	3.79(0.12)[a], 3.7(0.2)[b] 3.5(0.3)[c], 3.83(0.07)[d]	3.26
$z\,^6P^o$	3/2	3.819	3.71(0.12)[a], 3.6(0.2)[b] 3.4(0.3)[c]	3.25
$z\,^6D^o$	9/2	3.460	3.7(0.2)[b], 3.7(0.2)[c]	3.41
$z\,^6D^o$	7/2	3.487	3.75(20)[b], 3.8(0.3)[c] 3.68(0.7)[d]	3.43
$z\,^6D^o$	5/2	3.406	3.7(0.2)[h], 3.63(8)[d]	3.44
$z\,^6D^o$	3/2	3.392	3.7(0.2)[b], 3.7(0.2)[c] 3.83(10)[d]	3.45
$z\,^6D^o$	1/2	3.259	3.8(0.2)[b], 3.8(0.3)[c] 3.76(10)[d]	3.45
$z\,^6F^o$	11/2	2.982	3.2(0.2)[b], 3.3(0.2)[c] 3.19(4)[d]	2.83

State	J	τ (ns) Present	τ (ns) Expt	τ (ns) Kurucz
$z\,^6F^o$	9/2	3.024	3.2(0.2)[b], 3.24(6)[d]	2.89
$z\,^6F^o$	7/2	3.034	3.26 (10)[d]	2.92
$z\,^6F^o$	5/2	2.973	3.3(0.2)[c] 3.33(9)[d]	2.93
$z\,^6F^o$	3/2	2.908	3.3(0.2)[c], 3.34(10)[d]	2.94
$z\,^6F^o$	1/2	2.878	3.3(0.3)[c]	2.94
$z\,^4P^o$	5/2	3.250	3.44(0.11)[a]	
$z\,^4D^o$	7/2	2.476	3.02(0.07)[a], 3.1(0.2)[b]	2.43
$z\,^4D^o$	5/2	2.496	3.1(0.08)[a], 3.1(0.2)[b]	2.44
$z\,^4D^o$	3/2	2.494	3.0(0.2)[b]	2.43
$z\,^4D^o$	1/2	2.498	2.9(0.2)[b]	2.42
$z\,^4F^o$	9/2	3.471	3.87(0.09)[a], 3.7(0.2)[b]	3.34
$z\,^4F^o$	7/2	3.435	3.63(0.11)[a], 3.6(0.2)[b]	3.22
$z\,^4F^o$	5/2	3.417	3.75(0.14)[a], 3.7(0.2)[b]	3.26
$z\,^4F^o$	3/2	3.422	3.7(0.2)[b]	3.3

[a] Guo *et al* (1992).
[b] Hannaford *et al* (1992).
[c] Schade *et al* (1988).
[d] Biemont *et al* (1991).

selected oscillator strengths are presented for which a complete or almost complete set of fine structure oscillator strengths is available. There are a few measured values of Fe II that are with low uncertainty, rated B or <10%. However, most of them are rated with a 50% uncertainty (D in the NIST compilation). The measured f-values of the fine structure transitions of an *LS* multiplet usually do not correspond to the same experiment, rather to more than one experimental source. Among all the transitions, one complete set that has been rated with 10% uncertainty is a $^6D^e \rightarrow z\,^6D^o$. For this particular multiplet, the component fine structure transitions show about same level of agreement between the present values and the measured ones, as between the Kurucz values and the experimental values. However, overall comparison shows that the present values agree better with the measured values than the Kurucz data set. All the transitions listed in the NIST compilation have been compared, and this provides more detailed information on the uncertainties than the comparison of total *LS* multiplets. (The wavelengths given in table 4(*b*) are approximate.)

Another interesting comparison may be made between the calculated and observed lifetimes. We calculate the lifetime of a state based on all allowed transitions from the given state, i.e., $\tau_j = [\Sigma A_{ji}]^{-1}$ where $A_{ji} = \alpha^3 g_i / g_j E_{ji}^2 f_{ij} / \tau_0$ is the transition probability in s^{-1}, f_{ij} is the oscillator strength, τ_0 is the unit of time, and the sum is over all lower i-states that are connected by dipole allowed transitions from the upper state j. The lifetimes are calculated using the present fine structure f-values. Table 4(*c*) presents the calculated lifetimes and compares with the available measured values, and those from Kurucz. It should be noted that the Kurucz calculations involve forbidden transitions, and hence the lifetimes include both the dipole allowed and forbidden transitions; however the latter contribution is expected to be small for most levels under consideration. Present lifetimes of the fine structure levels of $z\,^6P^o$ agree well with the recent measured values of Hannaford *et al* (1992) and Guo *et al* (1992), whereas those of Schade *et al* (1988) are lower than the present values and other measured values. Values obtained by Kurucz are also lower than the present ones in a similar manner. For other states, the agreement between the present values and the experimental ones is better than that of Kurucz. The present values are in general within 5–10% of the experimental values.

4.3. Photoionization cross sections

Photoionization cross sections, including the detailed autoionizing resonances, are calculated for all bound states which include the 743 bound states of Fe II that lie below the first ionization threshold. Selected examples of the cross sections are presented. Figure 1 shows the photoionization cross sections of the $3d^5 4s\,^6D$ ground state of Fe II. As discussed by LeDourneuf *et al* (1993) the present ground state cross sections are about two orders of magnitude higher than the earlier calculations (Sawey and Berrington 1992) which included only the ground state of Fe III in the target expansion, whereas the dominant contribution stems from the photoionization of the 3d shell i.e. through coupling to the excited $3d^5 4s$ state of Fe III.

Figure 2(*a*) shows the photoionization cross sections of the lowest three quartet states, $3d^7(^4F)$, $3d^6 4s(^4D)$ and $3d^7(^4P)$. These metastable states are likely to be of considerable importance in astrophysical plasmas as one expects these to be in local thermodynamic equilibrium (LTE) even at fairly low densities owing to small radiative decay rates. Thus there may be significant populations in the low-lying metastable states,

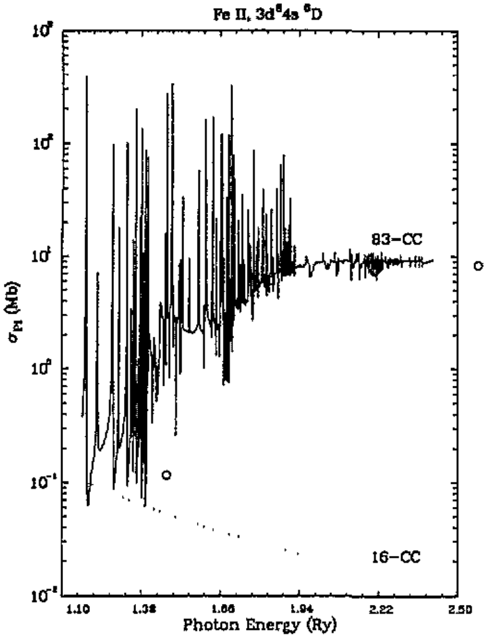

Figure 1. Photoionization cross section of the $3d^64s\ ^6D$ ground state of Fe II using 83-CC expansion. The dotted curve corresponds to earlier 16-CC calculations (Sawey and Berrington 1992); also shown are the central field cross sections in circles (Reilman and Manson 1979).

comparable to the ground state, in accordance with respective statistical weights. *Photoionization models therefore need to consider not only ground state photoionization but also that of at least these three states* (other states lie significantly higher and would be relatively less important). Figure 2(*b*) presents the photoionization cross sections of the three lowest doublet states of Fe II. Extensive resonances can be seen to dominate the metastable states $3d^7\ ^4P$ and $3d^7\ ^2P$ for the entire energy range up to the highest target threshold, and resulting in large variations in the background cross sections. Though the background cross sections smooth out at higher energies due to weaker coupling to high target states, all $3d^7$ states and $3d^64s\ ^4D$ show significant variations in the cross sections in the near threshold region due to resonances.

Figure 3 presents photoionization cross sections of two octet states, $3d^54s\ ^7S5s\ ^8S$ and the equivalent electron state $3d^54p^2\ ^8P$. Both states show the presence of a large resonance at the threshold, and the repetition of resonance patterns converging on to the $^7P^o$ target state. The octet state photoionization cross sections have been obtained for the first time.

Figure 4 consists of eight panels presenting photoionization cross sections of the Rydberg series of states, $3d^6\ ^5Dnp\ ^4P^o$ where $4 \leqslant n \leqslant 11$ of Fe II. The figure illustrates the wider photo-excitation of core (PEC) resonances which occur at the energies of the target states $3d^5\ ^6S4p\ (^5P^o)$, $3d^5\ ^4P4p(^5P^o)$, $3d^5\ ^4D4p\ (^5P^o)$, $3d^5\ ^4F4p(^5D^o)$, corresponding to dipole allowed transitions from the ground state ^5D (the positions of the PEC resonances are pointed out by arrows in the top panel). At these energies, the outer '*n*p' electron remains as a spectator while the ground core state $3d^54s\ ^5D$ is excited via strong dipole transitions giving rise to wide resonances in photoionization cross sections (Yu

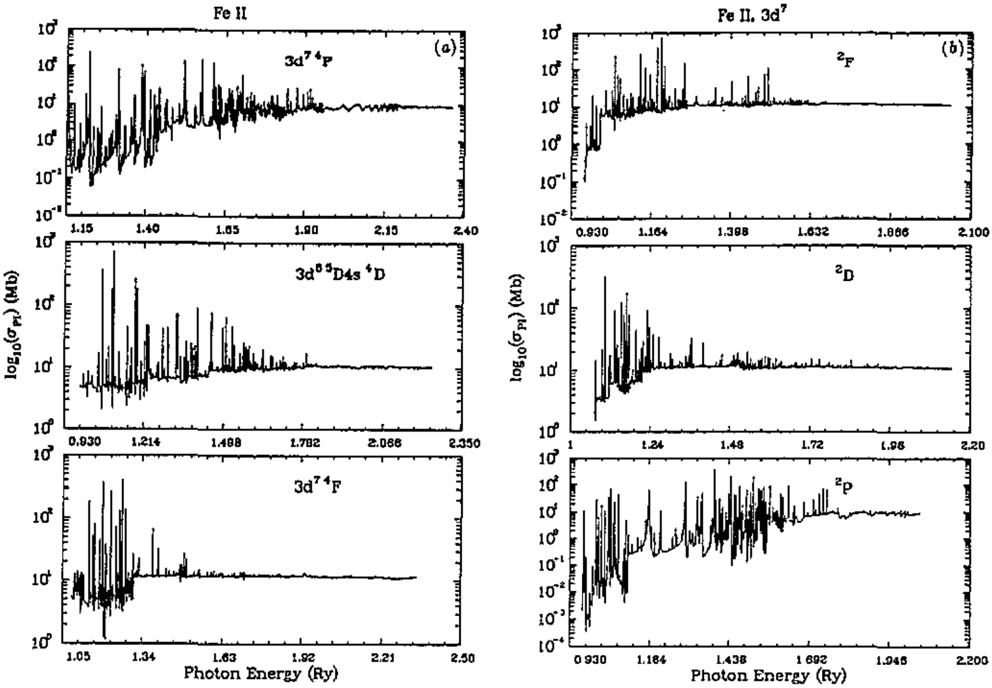

Figure 2. Photoionization cross sections of the metastable states of Fe II: (a) first three lowest quartet states, (b) three lowest doublet states.

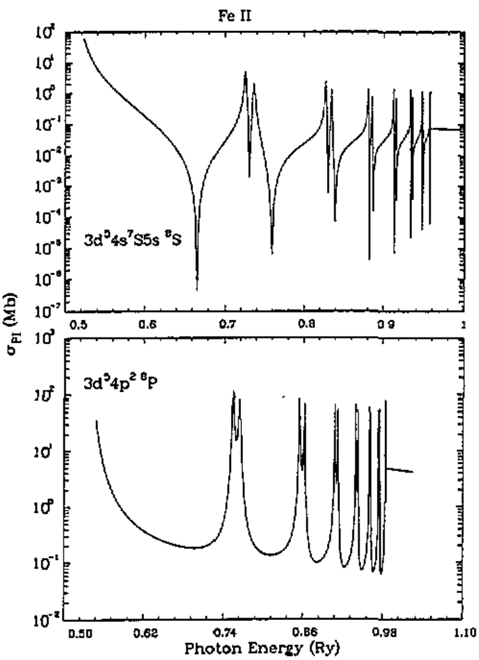

Figure 3. Photoionization cross sections of the two octet states, ^{8}S and ^{8}P, of Fe II.

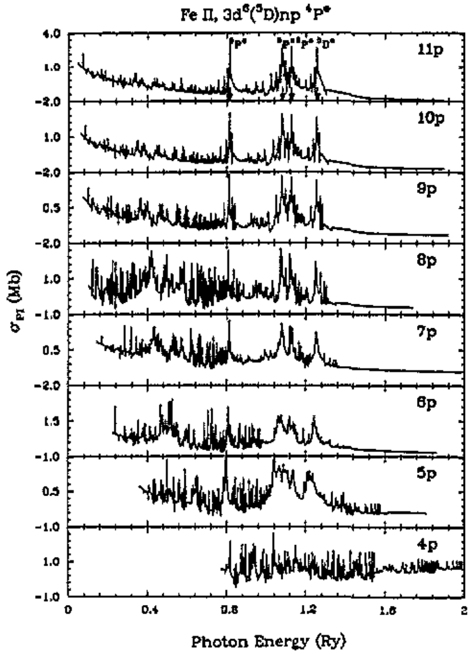

Figure 4. Photoionization cross sections of bound states along a Rydberg series, $3d^6(^5D)np\,^4P^o$, with $4 \leqslant n \leqslant 11$, illustrating photoexcitation-of-core (PEC) resonances.

and Seaton 1987). These resonances appear to be better resolved at higher excited states since the Rydberg resonances are usually weaker. The phenomenon of PEC resonances contradicts the usual assumptions of smooth hydrogenic behaviour of excited state photoionization cross sections, which may in fact be quite non-hydrogenic owing to the PEC features. It should be noted that even though there are more quintet states of Fe III in table 1 that are accessible through dipole transitions from the ground state, the figure shows only four since we treat several excited states to be degenerate as explained in section 3 and specified in the target states column of table 1.

4.4. *Monochromatic opacities*

The primary goal of the Opacity project is to calculate stellar opacities. Thus it is of some interest to examine the contribution to the opacities of a large calculation such as for Fe II reported herein. The total monochromatic opacity κ_ν is obtained on summing the contributions from all of the radiative processes such as bound–bound transitions, bound–free transitions, Thomson scattering, and free–free transitions (the former two are the main contributors). The theoretical steps involved in the opacities calculations are summarized by Seaton (1987). The contribution to the monochromatic opacity from a bound–bound transition is obtained as

$$\kappa_\nu = 2\pi^2 e^2/(mc) N_i f_{ij} \phi_\nu$$

where N_i is the number density of the ion, and ϕ_ν is a profile factor normalized to $\int \phi_\nu \, d\nu = 1$; and that of a bound–free transition is

$$\kappa_\nu = N_i \sigma_{PI}$$

where σ_{PI} is the photoionization cross section. In terms of the monochromatic opacities, the flow of radiation through a plasma is governed by the Rosseland mean defined as

$$\frac{1}{\kappa_R} = \int_0^\infty \frac{1}{\kappa_\nu} g(u)\, du \tag{1}$$

where

$$u = \frac{h\nu}{kT} \qquad g(u) = \frac{15}{4\pi^4} u^4 \frac{\exp(-u)}{[1-\exp(-u)]^3}.$$

The Rosseland mean is the weighted harmonic mean of the monochromatic opacities and κ_R is the Rosseland mean opacity. We have carried out separate calculations for the monochromatic and the mean opacities (using the OP code OPAC by Y Yu), for the single ion Fe II, with the new R-matrix data for the bound–bound and bound–free transitions from this work, and with the earlier R-matrix data of Sawey and Berrington (1992). At a temperature of 16 000 K and a density of 10^{16} cm^{-3}, we obtain values of κ_R to be 185 and 120 respectively, with the new and old data, resulting in an increase of over 50%. The detailed monochromatic opacity spectrum of Fe II, with the two data

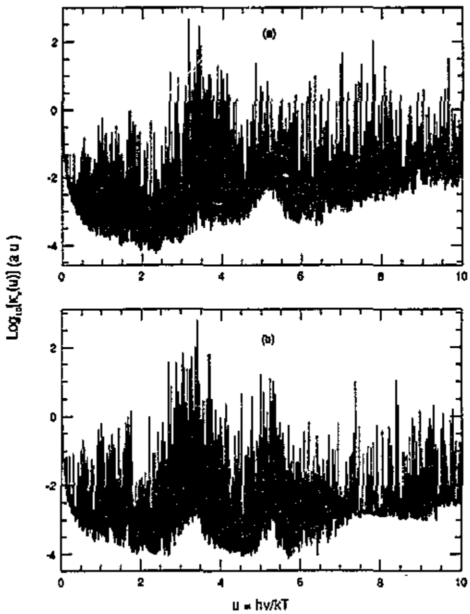

Figure 5. Monochromatic opacities, κ_ν, of Fe II at $\log T=4.2$ and $\log N_e=16$, (a) using the present radiative data and (b) the earlier data (Sawey and Berrington 1992).

sets, is shown in figure 5. In particular we note the rather large gap in the spectrum in the earlier data (bottom panel) around $u=3.5$ (5 eV), which has been filled in to a large extent by the new Fe II data (top panel). The Rosseland mean opacity, being a harmonic mean over the monochromatic opacities, is very sensitive to gaps or holes in the detailed spectrum, at low values of $h\nu/kT$ (equation (1)), and the feature in figure 5 is a significant contributor to the enhanced opacity. Also, in the high energy region, present opacities exhibit a rising trend and are more enhanced than those obtained using the earlier data.

4.5. Conclusion

Extensive radiative calculations for Fe II are described and it is expected that the new data will be applicable to a variety of astrophysical applications, in addition to the original aim of the calculations of accurate plasma opacities. The *LS* multiplet and fine structure oscillator strengths are compared with the available data and shown to be generally more accurate than other previous theoretical calculations (although there may be significant uncertainties for the weaker transitions). Most of the detailed photoionization data have been calculated for the first time. These are perhaps the largest close-coupling calculations carried out to date; yet we estimate that future relativistic calculations will be upto an order of magnitude more expensive in terms of computing resources and may not be feasible without massively parallel machines.

Acknowledgments

This work was partially supported by the National Science Foundation (PHY-9115057 and NASA LTSA program NAG W-3315). SNN aso acknowledges a research Fellowship by the College of Mathematical and Physical Sciences of the Ohio State University. The work was carried out on the Cray Y-MP at the Ohio Supercomputer Center (OSC). The authors are pleased to acknowledge the special allocation of memory and disk space by the OSC and the assistance of the staff in the execution of large jobs.

References

Allen C W 1976 *Astrophysical Quantities* 3rd edn (London: Athlone)
Berrington K A, Burke P G, Butler K, Seaton M J, Storey P J, Taylor K T and Yu Yan 1987 *J. Phys. B: At. Mol. Phys.* **20** 6379
Biemont E, Baudoux M, Kurucz R L, Ansbacher W, and Pinnington E H 1991, *Astron. Astrophys.* **249** 539
Eissner W, Jones M and Nussbaumer H 1974 *Comput. Phys. Commun.* **8** 270
Fuhr J R, Martin G A and Wiese W L 1988 *J. Phys. Chem. Ref. Data* **17** Suppl. 4
Guo B, Ansbacher W, Pinnington E H, Ji Q and Berends R W 1992 *Phys. Rev.* A **46** 641
Hannaford P, Lowe R M, Grevesse N and Noels A 1992 *Astron. Astrophys.* **259** 301
Johansson S 1992 Private communication
Kurucz R L 1981 *Semiempirical calculation of gf values: Fe II* (Smithsonian Astrophysical Observatory Special Report 390) (Cambridge, MA: Smithsonian Astrophysical Observatory)
Le Dourneuf M, Nahar S N and Pradhan A K 1993 *J. Phys. B: At. Mol. Opt. Phys* **26** L1
Moore C E 1952 *Atomic Energy Levels* vol II, NBS Circular No 487 (Washington, DC: US Govt. Printing Office)
Nahar S N and Pradhan A K 1991 *Phys. Rev.* A **44** 2935
Reilman R F and Manson S T 1979 *Astrophys. J. Suppl.* **40** 815
Sawey P M J and Berrington K A 1992 *J. Phys. B: At. Mol. Opt. Phys.* **25** 1451
Schade W, Mundt B and Helbig V 1988 *J. Phys. B: At. Mol. Opt. Phys.* **21** 2691
Seaton M J 1987 *J. Phys. B: At. Mol. Phys.* **20** 6363
Smith P L and Whaling W 1973 *Astrophys. J.* **183** 313
Sugar J and Corliss C 1985 *J. Phys. Chem. Ref. Data* **14** Suppl. 2
Yu Yan and Seaton M J 1987 *J. Phys. B: At. Mol. Phys.* **20** 6409